Quantum Selection of Order in an *XXZ* Antiferromagnet on a Kagome Lattice

A. L. Chernyshev[1] and M. E. Zhitomirsky[2]
[1]*Department of Physics and Astronomy, University of California, Irvine, California 92697, USA*
[2]*Service de Physique Statistique, Magnétisme et Supraconductivité, UMR-E9001 CEA-INAC/UJF, 17 rue des Martyrs, 38054 Grenoble Cedex 9, France*

(Received 22 September 2014; revised manuscript received 22 October 2014; published 3 December 2014)

Selection of the ground state of the kagome-lattice *XXZ* antiferromagnet by quantum fluctuations is investigated by combining nonlinear spin-wave and real-space perturbation theories. The two methods unanimously favor $\mathbf{q} = 0$ over $\sqrt{3} \times \sqrt{3}$ magnetic order in a wide range of the anisotropy parameter $0 \leq \Delta \lesssim 0.72$. Both approaches are also in accord on the magnitude of the quantum order-by-disorder effect generated by topologically nontrivial, looplike spin-flip processes. A tentative S-Δ phase diagram of the model is proposed.

DOI: 10.1103/PhysRevLett.113.237202 PACS numbers: 75.10.Jm, 75.30.Ds, 75.45.+j, 75.50.Ee

Kagome-lattice antiferromagnets (KGAFMs) are central to theoretical and experimental studies in frustrated magnets. They host long-sought magnetically disordered spin liquids and intriguing valence-bond solids, exhibit order-by-disorder phenomena, and are dominated by unconventional excitations [1–26]. Many of these remarkable properties take their root in a massive degeneracy of the ground state of the classical kagome nearest-neighbor Heisenberg model. The degeneracy can be lifted by thermal or quantum fluctuations, or by secondary interactions. Because of experimental realizations, order selection by the symmetry-breaking Dzyaloshinskii-Moriya (DM) terms has been intensely studied [27–35] and so has been the effect of further-neighbor couplings [2], which lift the degeneracy within the manifold of classical 120° states. Two of such states, the $\sqrt{3} \times \sqrt{3}$ and the $\mathbf{q} = 0$ spin patterns, are the main contenders for the ground state from the quasiclassical perspective [36], see Figs. 1(a) and 1(b).

On the other hand, studies of quantum effects have been concentrated on the Heisenberg case where most methods offer only limited insight into how the ground state is selected. In this Letter, we address the problem of order by disorder (OBD) by quantum fluctuations in KGAFMs using the *XXZ* version of the nearest-neighbor, spin-S model

$$\hat{\mathcal{H}} = J \sum_{\langle ij \rangle} (S_i^x S_j^x + S_i^y S_j^y + \Delta S_i^z S_j^z), \qquad (1)$$

where anisotropy is of the easy-plane type, $0 < \Delta < 1$. It is important to note that the degeneracy among the 120° coplanar states of the classical *XXZ* KGAFM remains the same as in the Heisenberg limit, $\Delta = 1$. Therefore, by extending the parameter space without explicitly lifting degeneracy of the classical ground-state manifold we are able to provide deeper insight into the quantum OBD effect. More specifically, we shed light on the mechanism by which the choice is made between $\mathbf{q} = 0$ and $\sqrt{3} \times \sqrt{3}$ ordered patterns in KGAFMs and present a rare example of the situation when quantum OBD defies the general trend and yields the ground state that is different from the one favored by thermal fluctuations.

On the technical side, we take advantage of the fact that the so-called "flat mode," the branch of localized linear spin-wave excitations which has zero energy in the Heisenberg limit, see Fig. 1(c), becomes gaped for $\Delta < 1$ with $\varepsilon_{\mathbf{k}} \propto \sqrt{1 - \Delta}$, see Fig. 1(d). Because of that, a controlled $1/S$ expansion becomes possible in the *XXZ* KGAFM, allowing for a detailed investigation of the quantum selection of the ordered state [37].

Another method that allows for an effective treatment of the highly degenerate frustrated spin systems is the real-space perturbation theory (RSPT). Applied to the KGAFMs, it operates directly within the manifold of

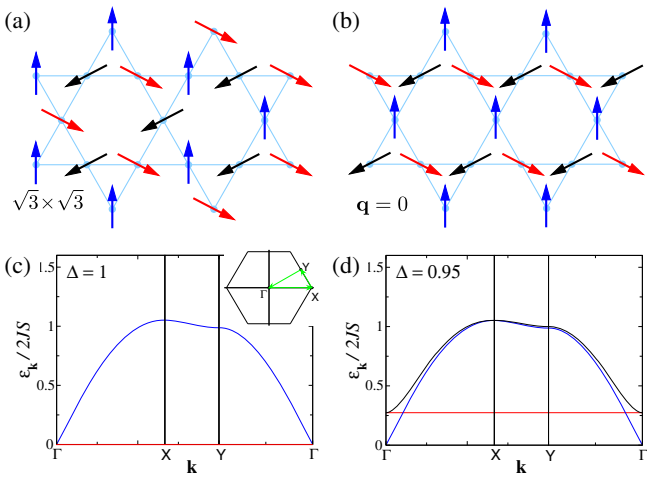

FIG. 1 (color online). (a) $\sqrt{3} \times \sqrt{3}$ and (b) $\mathbf{q} = 0$ spin configurations. Dispersions of spin excitations within the harmonic approximation for (c) $\Delta = 1$ and (d) $\Delta = 0.95$.

classical 120° states and, by analyzing terms of various order of the perturbation, creates an intuitively transparent real-space hierarchy of effective couplings that are responsible for the ground-state selection. As we show below, it is the convolution of the two methods, $1/S$ expansion and RSPT, which is especially insightful.

Nonlinear spin-wave theory (SWT).—For any ordered state from the coplanar 120° manifold one can rewrite (1) in a rotating local basis as

$$\hat{\mathcal{H}} = J\sum_{\langle ij\rangle}[\Delta S_i^y S_j^y + \cos\theta_{ij}(S_i^x S_j^x + S_i^z S_j^z) + \sin\theta_{ij}(S_i^z S_j^x - S_i^x S_j^z)], \quad (2)$$

where $\theta_{ij} = \theta_i - \theta_j$. Clearly, it is only the last term in (2) which is able to distinguish between different 120° spin configurations by virtue of containing $\sin\theta_{ij} = \pm\sqrt{3}/2$ for the clockwise or counterclockwise spin rotation. This term corresponds to the nonlinear, cubic coupling of spin waves and does not contribute to the linear SWT. Consider the $1/S$ expansion of the ground-state energy

$$E = E_{\rm cl} + \langle\mathcal{H}_2\rangle + \langle\mathcal{H}_4\rangle + \delta E^{(3)} + \ldots, \quad (3)$$

where the first term is the classical energy $\mathcal{O}(S^2)$, the second is the linear SWT correction $\mathcal{O}(S)$, and the last two are the contribution of the quartic and cubic terms, both $\mathcal{O}(1)$. It is easy to see from (2) that quartic terms are also unable to differentiate between 120° structures, leaving the cubic term as a sole source of the quantum OBD effect to this $1/S$ order. The energy correction from the cubic terms is represented by the diagram in the lower inset of Fig. 2 and is given by

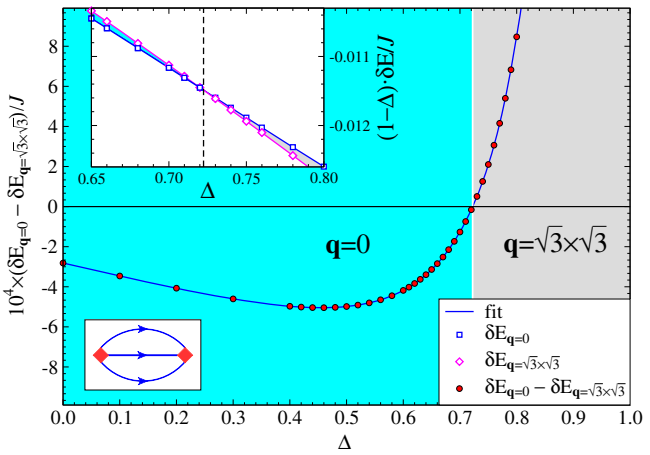

FIG. 2 (color online). Difference of the ground-state energies (3) of the $\mathbf{q}=0$ and $\sqrt{3}\times\sqrt{3}$ states, per spin. Upper inset: energy correction $\delta E^{(3)}$ for the $\mathbf{q}=0$ (squares) and $\sqrt{3}\times\sqrt{3}$ (diamonds) states. The dashed line marks the transition. Lower inset: diagram for $\delta E^{(3)}$ term in the energy expansion.

$$\delta E^{(3)} = -\frac{1}{6N}\sum_{\nu\mu\eta}\sum_{\mathbf{q},\mathbf{k}}\frac{|V^{\nu\mu\eta}_{\mathbf{q},\mathbf{k},-\mathbf{k}-\mathbf{q}}|^2}{\varepsilon^{\nu}_{\mathbf{q}} + \varepsilon^{\mu}_{\mathbf{k}} + \varepsilon^{\eta}_{-\mathbf{k}-\mathbf{q}}}, \quad (4)$$

where ν,μ,η numerate spin-wave branches with harmonic energies $\varepsilon^{\alpha}_{\mathbf{k}}$ and the cubic vertex comes from the anharmonic part of the spin-wave Hamiltonian

$$\hat{\mathcal{H}}_3 = \frac{1}{3!}\sum_{\nu\mu\eta}\sum_{\mathbf{q},\mathbf{k}} V^{\nu\mu\eta}_{\mathbf{q},\mathbf{k},-\mathbf{k}-\mathbf{q}} b^{\dagger}_{\nu,\mathbf{q}} b^{\dagger}_{\mu,\mathbf{k}} b^{\dagger}_{\eta,-\mathbf{k}-\mathbf{q}} + \text{H.c.} \quad (5)$$

As is clear from previous discussion, this vertex has a different form for different ordered structures and should be obtained from the spin-wave expansion for each specific 120° spin pattern.

For the linear SWT of the XXZ model (2), we generalize the approach of [2], which has suggested a two-step diagonalization procedure consisting of the unitary transformation of the unit-cell bosons followed by the Bogolyubov transformation for each mode. With that we are able to obtain cubic vertices (5) for the $\mathbf{q}=0$ and $\sqrt{3}\times\sqrt{3}$ states in a fully analytic and elegant form [38], which permit high-accuracy numerical integration in (4) and allow us to study quantum OBD effect. The results of such calculations are presented in Fig. 2.

Our main result is the quantum selection of the $\mathbf{q}=0$ state over the $\sqrt{3}\times\sqrt{3}$ counterpart for anisotropy values extending from the XY limit, $\Delta=0$, to the transition point $\Delta_c \approx 0.722\,35$. This is contrary to the common belief that quantum fluctuations follow the same selection trend as thermal ones [40]. Indeed, the asymptotic selection of the $\sqrt{3}\times\sqrt{3}$ magnetic structure by thermal fluctuations for the classical KGAFM in both the Heisenberg [2,36,41] and the XY limits [42–44] shows no change in the ordering pattern as a function of Δ in contrast to the behavior of the quantum model in Fig. 2. Although the $1/S$ energy correction diverges as $(1-\Delta)^{-1}$, signifying a failure of the expansion for $\Delta\to 1$, our results leave little doubt that the $\sqrt{3}\times\sqrt{3}$ state should remain the ground state in the entire range $\Delta_c < \Delta \le 1$. Previously, a self-consistent spin-wave treatment of the Heisenberg limit [4] has provided indirect evidence in favor of the $\sqrt{3}\times\sqrt{3}$ ground state for $S\gg 1$. Here, this result is strongly implied by a direct calculation of the ground-state energy. Last, we observe that the energy gain from the quantum OBD effect is only a fraction of $10^{-3}J$ per spin.

Real-space perturbation theory.—What is the mechanism of quantum selection of the ground state? We address this question using the RSPT [45–48]. This approach divides the Hamiltonian (2) into an unperturbed part $\hat{\mathcal{H}}_0 = h\sum_i(S - S_i^z)$, describing spin fluctuations in the local field $h = 2JS$, and perturbation $\hat{V}$, which couples fluctuations on adjacent sites. Then, the standard perturbation theory is used to calculate quantum corrections to the classical ground-state energy. The

coupling between spin fluctuations contains four terms $\hat{V} = \sum_{i,j}(\hat{V}_1^{ij} + \hat{V}_2^{ij} + \hat{V}_3^{ij} + \hat{V}_4^{ij})$:

$$\hat{V}_1^{ij} = -A_+(S_i^+ S_j^+ + \text{H.c.}), \qquad \hat{V}_2^{ij} = 2A_- S_i^+ S_j^-,$$
$$\hat{V}_3^{ij} = -B_{ij}\delta S_i^z (S_j^+ + S_j^-), \qquad \hat{V}_4^{ij} = -C\delta S_i^z \delta S_j^z, \tag{6}$$

where we introduce $\delta S_i^z = S - S_i^z$, $A_\pm = J(\Delta \pm 1/2)/8$, $B_{ij} = J\sin\theta_{ij}/2$, $C = J/4$, and keep $\sin\theta_{ij} = \pm\sqrt{3}/2$ in $\hat{V}_3$ explicit, see [38] for details. The first three terms in (6) can be referred to as double spin flip, spin-flip hopping, and single spin flip, the latter being a descendant of the cubic term (2). As in the $1/S$ expansion, this is the only term which is sensitive to the 120° pattern and, therefore, is the key to the selection of the ground state.

Since every term in the energy expansion corresponds to a finite cluster of spins coupled by perturbations in (6) and since the classical ground state is a vacuum for spin flips, contributions that are relevant to lifting the ground-state degeneracy must begin and end with a double spin flip and must also contain a pair of single spin flips. The first process of such kind appears in the fourth order, an example given by the operator sequence $\hat{V}_1^{12} \to \hat{V}_3^{13} \to \hat{V}_3^{12} \to \hat{V}_1^{13}$ shown in Fig. 3(a). The respective energy shift depends on the mutual orientation of $\mathbf{S}_2$ and $\mathbf{S}_3$ because $\delta E^{(4)} \propto \sin\theta_{12}\sin\theta_{13}$. However, an obvious symmetry leaves the degeneracy intact at this order of expansion, because for any coupling between $\mathbf{S}_2$ and $\mathbf{S}_3$ there is a "mirror" process that couples identically $\mathbf{S}_2$ with $\mathbf{S}_{3'}$, see Fig. 3(b), providing the same energy gain to both the $\sqrt{3}\times\sqrt{3}$ and the $\mathbf{q} = 0$ states.

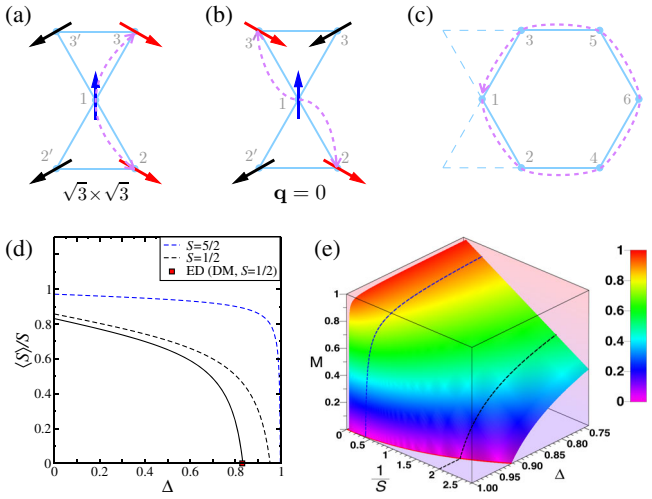

FIG. 3 (color online). (a),(b) Schematics of the symmetry related processes of the fourth order. (c) Topologically nontrivial path of the seventh order. (d) Magnetization $M = \langle S\rangle/S$ vs Δ in linear SWT for $S = 1/2$ and $S = 5/2$, dashed lines. Solid line, a sketch of $M(\Delta)$ for the case of DM interaction. (e) Linear SWT result for $M(S, \Delta)$.

Generalizing this trend, we conclude that the degeneracy-lifting terms must correspond to linked clusters of a nontrivial topology, with the smallest cluster consisting of a hexagon loop and generated by the seventh-order process depicted in Fig. 3(c). One example of the operator sequence is given by $\hat{V}_1^{24} \to \hat{V}_3^{21} \to \hat{V}_3^{13} \to \hat{V}_1^{12} \to \hat{V}_1^{56} \to \hat{V}_1^{46} \to \hat{V}_1^{35}$ and contains five double flips and two single flips. This type of process yields the only relevant seventh-order contribution at $\Delta = 1/2$, for which the amplitude A_- of the spin-flip hopping $\hat{V}_2$ (6) vanishes together with the rest of the degeneracy-lifting terms. The energy correction at $\Delta = 1/2$ corresponds to an effective antiferromagnetic coupling between the second-neighbor spins $\mathbf{S}_2$ and $\mathbf{S}_3$, $\delta E^{(7)} \sim +\sin\theta_{12}\sin\theta_{13}$ [38], favoring the $\mathbf{q} = 0$ state.

Moreover, one can show that for $\Delta < 1/2$ all relevant seventh-order processes have the same sign and also favor the $\mathbf{q} = 0$ state. For $\Delta > 1/2$, some of the terms switch sign. This implies that the transition to the $\sqrt{3}\times\sqrt{3}$ state can take place only at some $\Delta_c > 1/2$, in agreement with the the nonlinear SWT result $\Delta_c \approx 0.72$.

There are close parallels between the nonlinear SWT and the real-space approach. Although the degeneracy-lifting contribution in the RSPT is of the seventh order, it is still of the second order in cubic terms, the same as in the nonlinear SWT (4). More importantly, the high order of the relevant perturbation processes explains the smallness of the quantum OBD effect. Essentially, the RSPT is an expansion in $1/z$, where z is the coordination number, which gives the right order-of-magnitude estimate for the seventh-order effect $\delta E \sim 10^{-4}J$. A more careful calculation using the actual perturbation terms in (6) and combinatorial factors of different processes of seventh order gives a similar answer [38]. Our conclusion on the topological nature of the effective exchange responsible for the ground-state selection also makes it extremely unlikely that a state with an extended unit cell can compete with the ones considered in this work.

Phase diagram.—We now construct the phase diagram of the XXZ KGAFM (1) as a function of anisotropy Δ and spin S. For that, we calculate the ordered moment within the harmonic SWT approximation, $\langle S\rangle = S - \langle a_i^\dagger a_i\rangle$, to map out the extent of the magnetically ordered state. Because of the degeneracy of classical 120° states, the harmonic spin-wave spectrum is identical in all of them and yields the same result. Here we simply estimate stability of the Neél order with respect to the "diagonal" quantum fluctuation for a given state. While this analysis completely neglects the "off-diagonal" tunneling within the manifold, such processes should be exponentially suppressed for larger spins [49].

Figure 3(d) shows magnetization $M = \langle S\rangle/S$ vs Δ for two representative values of the spin. The Neél state is stabilized already at rather small $1 - \Delta_c' \approx 0.05$ for $S = 1/2$ and $1 - \Delta_c' \approx 0.002$ for $S = 5/2$. Considering spin S as a continuous variable, we plot $M(S, \Delta)$ in Fig. 3(e) where

dashed lines are the same as in Fig. 3(d) and the color is for the magnitude of M. The $M = 0$ curve is the Neél order phase boundary in the S-Δ plane, see also Fig. 4(a). Simple algebra yields an asymptotic expression for it, $1 - \Delta_c' \approx (96S^2)^{-1}$, which agrees exceedingly well with the results of numerical integration [38].

In Fig. 3(d) we also sketch results of the exact diagonalization (ED) for $S = 1/2$ KGAFM with the out-of-plane DM term [33], which selects a $\mathbf{q} = 0$ ground state but yields a harmonic Hamiltonian identical to the XXZ case with rescaling $1 - \Delta \Leftrightarrow \sqrt{3}D_z$ [31,37,50]. Since the DM term suppresses tunneling processes within the manifold, it is reasonable to compare ED with SWT results to evaluate the accuracy of the SWT Neél order boundary. For the latter, one can see a qualitative agreement with ED and a quantitative exaggeration of the extent of the ordered phase, expected for the SWT approach.

We now combine our SWT results in Fig. 4(a), which shows the S-Δ phase diagram. The solid line is the linear SWT result for the Neél order boundary $\langle S \rangle = 0$, see also Fig. 3(e), and the dashed line is its asymptotic approximation mentioned above. As we discussed, the harmonic treatment gives a good qualitative idea for the phase boundary between magnetically ordered and disordered phases, but does not specify which of the 120° Neél states is chosen. We infer this information from the nonlinear SWT results in Fig. 2 and complete our perturbative S-Δ phase diagram by adding the boundary between the $\mathbf{q} = 0$ and $\sqrt{3} \times \sqrt{3}$ states.

There are two trends that are not included in this phase diagram and are beyond the methods used in the current work. The nonlinear SWT approach is a perturbative treatment of the quantum OBD effect, which fails in the vicinity of the Heisenberg limit. However, it is known that

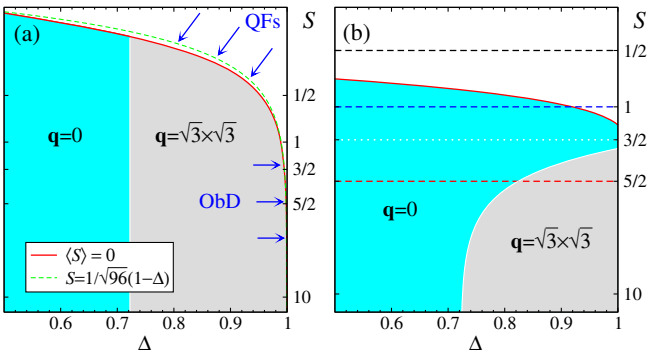

FIG. 4 (color online). (a) S-Δ phase diagram, S is on the logarithmic scale. The solid line is the Neél order boundary $\langle S \rangle = 0$ from the linear SWT; the dashed line is its asymptotic approximation. The vertical boundary between $\mathbf{q} = 0$ and $\sqrt{3} \times \sqrt{3}$ states is from the nonlinear SWT. (b) Tentative S-Δ phase diagram. Suppression of magnetic order by quantum fluctuations (QFs) and quantum OBD near the Heisenberg limit are suggested. Horizontal lines are cuts for different values of the spin.

quantum OBD should extend the Neél-ordered region of the phase diagram to the $\Delta = 1$ axis for larger spin values. It has been argued by the self-consistent version of SWT [4] that $\sqrt{3} \times \sqrt{3}$ is the ground state of the Heisenberg KGAFM for $S \gg 1$.

The other trend is the suppression of the Neél order by quantum fluctuations for smaller spins, leading to the growth of the nonmagnetic region of the phase diagram. As was argued recently by several groups using numerical approaches [51–53], the $S = 1/2$ XXZ KGAFM remains in a spin-liquid state for the entire range of $\Delta \leq 1$. Our results for the $S = 1/2$ case in Fig. 4(a) are, therefore, inadequate, most likely because of the neglect of the tunneling between different states in the 120° manifold.

In order to capture some of these trends, we modify the mean-field condition $\langle S \rangle = 0$ used above by including the self-consistently renormalized spin-wave dispersion of the "flat mode" for the Heisenberg limit from [4]. While this is not an entirely rigorous procedure, it should provide a reasonable estimate on the extent of the region of stability due to quantum OBD for $\Delta = 1$. The resulting values for the "critical" S_c, above which the system orders magnetically, come out as $S_c^{\mathbf{q}=0} \approx 0.17$ and $S_c^{\sqrt{3}\times\sqrt{3}} \approx 0.18$. While, obviously, this is another case of quantitative exaggeration of the extent of the ordered phase by an SWT approach, this estimate makes it extremely unlikely that the Heisenberg KGAFM with $S \gtrsim 1$ will be magnetically disordered. In fact, recent numerical work [17] has indicated that the Heisenberg KGAFMs with $S \geq 3/2$ all order in a $\sqrt{3} \times \sqrt{3}$ configuration.

Combining these trends, we propose a tentative S-Δ phase diagram of the nearest-neighbor XXZ KGAFM model in Fig. 4(b). In the Heisenberg limit, for larger values of spin the ground state is the $\sqrt{3} \times \sqrt{3}$ state, which switches to $\mathbf{q} = 0$ upon reducing Δ. For $S = 1$ the same trajectory begins with the magnetically disordered state and the system enters directly into the $\mathbf{q} = 0$ state. As shown by the recent numerical results, $S = 1/2$ remains quantum disordered for the entire range of Δ. Finally, there may or may not exist an intermediate value of spin for which the Heisenberg limit is already in the $\mathbf{q} = 0$ domain and no transition occurs versus Δ. While predictions of this work are firm for the larger values of spin, the ultimate answer on the exact sequence of phases for smaller spins should be sought via numerical approaches.

Conclusions.—By advancing the nonlinear $1/S$ expansion and the real-space perturbation theory we investigated quantum order-by-disorder selection of the ground state of the nearest-neighbor XXZ antiferromagnet on the kagome lattice. We demonstrated that the order selection is generated by topologically nontrivial tunneling processes, presented strong evidence of the rare case of quantum and thermal fluctuations favoring different ground states, proposed a tentative S-Δ phase diagram of the model, and suggested further studies.

We acknowledge useful discussions with C. Batista, F. Becca, A. V. Chubukov, G. Jackeli, A. Läuchli, R. Moessner, N. Perkins, S. Parameswaran, H. Tsunetsugu, and S. R. White. Work by A. L. C. was supported by the U.S. Department of Energy, Office of Science, Basic Energy Sciences under Award No. DE-FG02-04ER46174. A. L. C. would like to thank the Aspen Center for Physics, where part of this work was done, for their hospitality. The work at Aspen was supported in part by NSF Grant No. PHYS-1066293.

[1] C. Zeng and V. Elser, Phys. Rev. B **42**, 8436 (1990).
[2] A. B. Harris, C. Kallin, and A. J. Berlinsky, Phys. Rev. B **45**, 2899 (1992).
[3] J. T. Chalker, P. C. W. Holdsworth, and E. F. Shender, Phys. Rev. Lett. **68**, 855 (1992).
[4] A. Chubukov, Phys. Rev. Lett. **69**, 832 (1992); J. Appl. Phys. **73**, 5639 (1993).
[5] S. Sachdev, Phys. Rev. B **45**, 12377 (1992).
[6] J. T. Chalker and J. F. G. Eastmond, Phys. Rev. B **46**, 14201 (1992).
[7] R. R. P. Singh and D. A. Huse, Phys. Rev. Lett. **68**, 1766 (1992).
[8] P. Lecheminant, B. Bernu, C. Lhuillier, L. Pierre, and P. Sindzingre, Phys. Rev. B **56**, 2521 (1997).
[9] M. Mambrini and F. Mila, Eur. Phys. J. B **17**, 651 (2000).
[10] P. Nikolic and T. Senthil, Phys. Rev. B **68**, 214415 (2003).
[11] R. R. P. Singh and D. A. Huse, Phys. Rev. B **76**, 180407(R) (2007).
[12] J. S. Helton, K. Matan, M. P. Shores, E. A. Nytko, B. M. Bartlett, Y. Yoshida, Y. Takano, A. Suslov, Y. Qiu, J.-H. Chung, D. G. Nocera, and Y. S. Lee, Phys. Rev. Lett. **98**, 107204 (2007).
[13] T.-H. Han, J. S. Helton, S. Chu, D. G. Nocera, J. A. Rodriguez-Rivera, C. Broholm, and Y. S. Lee, Nature (London) **492**, 406 (2012).
[14] K. Matan, T. Ono, Y. Fukumoto, T. J. Sato, J. Yamaura, M. Yano, K. Morita, and H. Tanaka, Nat. Phys. **6**, 865 (2010).
[15] K. Matan, Y. Nambu, Y. Zhao, T. J. Sato, Y. Fukumoto, T. Ono, H. Tanaka, C. Broholm, A. Podlesnyak, and G. Ehlers, Phys. Rev. B **89**, 024414 (2014)
[16] S. Yan, D. A. Huse, and S. R. White, Science **332**, 1173 (2011).
[17] O. Götze, D. J. J. Farnell, R. F. Bishop, P. H. Y. Li, and J. Richter, Phys. Rev. B **84**, 224428 (2011).
[18] L. Balents, Nature (London) **464**, 199 (2010).
[19] Y. Iqbal, F. Becca, S. Sorella, and D. Poilblanc, Phys. Rev. B **87**, 060405 (2013).
[20] H. J. Changlani and A. M. Läuchli, arXiv:1406.4767.
[21] T. Liu, W. Li, A. Weichselbaum, J. von Delft, and G. Su, arXiv:1406.5905.
[22] S. Nishimoto and M. Nakamura, arXiv:1409.5870.
[23] I. Rousochatzakis, Y. Wan, Oleg Tchernyshyov, and F. Mila, Phys. Rev. B **90**, 100406(R) (2014).
[24] Z. Hao and O. Tchernyshyov, Phys. Rev. B **81**, 214445 (2010).
[25] Y. Wan and O. Tchernyshyov, Phys. Rev. B **87**, 104408 (2013).
[26] M. Taillefumier, J. Robert, C. L. Henley, R. Moessner, and B. Canals, Phys. Rev. B **90**, 064419 (2014).
[27] A. Zorko, S. Nellutla, J. van Tol, L. C. Brunel, F. Bert, F. Duc, J.-C. Trombe, M. A. de Vries, A. Harrison, and P. Mendels, Phys. Rev. Lett. **101**, 026405 (2008).
[28] A. Zorko, F. Bert, A. Ozarowski, J. van Tol, D. Boldrin, A. S. Wills, and P. Mendels, Phys. Rev. B **88**, 144419 (2013).
[29] K. Matan, D. Grohol, D. G. Nocera, T. Yildirim, A. B. Harris, S. H. Lee, S. E. Nagler, and Y. S. Lee, Phys. Rev. Lett. **96**, 247201 (2006).
[30] H. Yoshida, Y. Michiue, E. Takayama-Muromachi, and M. Isobe, J. Mater. Chem. **22**, 18793 (2012).
[31] T. Yildirim and A. B. Harris, Phys. Rev. B **73**, 214446 (2006).
[32] M. Elhajal, B. Canals, and C. Lacroix, Phys. Rev. B **66**, 014422 (2002).
[33] O. Cépas, C. M. Fong, P. W. Leung, and C. Lhuillier, Phys. Rev. B **78**, 140405 (2008).
[34] L. Messio, O. Cépas, and C. Lhuillier, Phys. Rev. B **81**, 064428 (2010).
[35] Y. Huh, L. Fritz, and S. Sachdev, Phys. Rev. B **81**, 144432 (2010).
[36] J. N. Reimers and A. J. Berlinsky, Phys. Rev. B **48**, 9539 (1993).
[37] We note that there exists a close similarity of the harmonic part of the XXZ model and the kagome Hamiltonian with the out-of-plane DM interaction D_z. However, in the latter case the ground state is selected on a classical level. In that sense, XXZ anisotropy is a much lighter perturbation, as it does not lift the macroscopic degeneracy between the manifold of 120° states and allows us to study a purely quantum OBD mechanism.
[38] See Supplemental Material at http://link.aps.org/supplemental/10.1103/PhysRevLett.113.237202, which includes Ref. [39], for details of theoretical calculations for the kagome antiferromagnet.
[39] R. J. Baxter, J. Math. Phys. (N.Y.) **11**, 784 (1970).
[40] Thus, for the values of $\Delta < \Delta_c \approx 0.72$, one can expect a transition, as a function of T, between the quantum-fluctuation-dominated $\mathbf{q} = 0$ correlations to thermal-fluctuation-dominated $\sqrt{3} \times \sqrt{3}$ correlations. While the transition is likely to be of the first order, this is a matter for future investigation.
[41] C. L. Henley, Phys. Rev. B **80**, 180401(R) (2009).
[42] D. A. Huse and A. D. Rutenberg, Phys. Rev. B **45**, 7536(R) (1992).
[43] S. E. Korshunov, Phys. Rev. B **65**, 054416 (2002).
[44] M. S. Rzchowski, Phys. Rev. B **55**, 11745 (1997).
[45] M. W. Long, J. Phys. Condens. Matter **1**, 2857 (1989).
[46] M. T. Heinilä and A. S. Oja, Phys. Rev. B **48**, 7227 (1993).
[47] B. Canals and M. E. Zhitomirsky, J. Phys. Condens. Matter **16**, S759 (2004).
[48] D. L. Bergman, R. Shindou, G. A. Fiete, and L. Balents, Phys. Rev. B **75**, 094403 (2007).
[49] J. von Delft and C. L. Henley, Phys. Rev. B **48**, 965 (1993).
[50] R. Ballou, B. Canals, M. Elhajal, C. Lacroix, and A. Wills, J. Magn. Magn. Mater. **262**, 465 (2003).
[51] A. M. Läuchli (private communication).
[52] S. R. White (unpublished).
[53] Y.-C. He and Y. Chen, arXiv:1407.2740.